ELSEVIER

Electrical Power & Energy Systems Vol. 18, No. 2, pp. 81–97, 1996

0142-0615(94)00003-4
0142-0615/96/$15.00 + 0.00

Investigations of load–tap changer interaction

D Popović
Department of Electrical Engineering,
University of Sydney, Building J13,
NSW 2006, Australia

I A Hiskens
Department of Electrical and Computer Engineering,
The University of Newcastle, University Drive,
Callaghan, NSW 2308, Australia

D J Hill
Department of Electrical Engineering,
University of Sydney, Building J13,
NSW 2006, Australia

This paper explores the dynamic behaviour of loads and tap changers during the process of voltage collapse in power systems. Using an exponential recovery load model representing the dynamic behaviour of aggregate loads, the mechanism of voltage collapse is illustrated. Dynamic interaction between loads and transformers is investigated. Based on such dynamic considerations, a tap locking strategy is proposed which ensures that voltage collapse does not occur. Investigations focus on determining a critical value of tap position such that locking at a smaller value of tap results in stable behaviour, but locking at a larger value results in voltage collapse.

Keywords: voltage stability, voltage control, tap locking, load modeling

I. Introduction

Owing to the number of widespread system black-outs throughout the world the study of voltage instability problems has become an important and interesting area of research and studies. Voltage collapse is usually characterized by a progressive fall of voltages and shortage of reactive power reserves in the network. Primary events which can induce voltage collapse are line or generator tripping, sudden increase in load, and limiting or loss of reactive power support. Depending on the severity of the contingency, the voltage collapse time frame could range from seconds to minutes. Despite an enormous research effort, a number of aspects of the dynamics of voltage collapse are still not well understood.

The voltage collapse phenomenon can be related to the action of tap changers on transformers, reactive power limiting protection at generators and load characteristics at low voltage magnitudes[1–3,5,6,9,13]. These devices can interact in quite a complicated way. Many investigations of the mechanisms of voltage collapse have shown that tapping of transformers to restore voltages in an already weakened system could cause further voltage reduction[2,4]. This is a consequence of the transformers higher reactive demands in that case. If that reactive power could not be adequately supplied, either because of network constraints, or because of generators encountering reactive power limits, then voltages would fall further. Further tapping would cause further voltage falls, until ultimately protection action would result in cascaded tripping of system components, or machines would separate because of the inability of the network to maintain an adequate level of synchronizing torque.

Because voltage collapse usually occurs on heavily loaded systems, and tends to result in abnormal voltage behaviour at load buses, load–voltage characteristics are considered to be a very important factor. Further, dynamic behaviour of loads is important[6–8,12,13]. The load at transmission levels is an aggregation of various load devices, each with some dynamic attribute. A general dynamic load modelling methodology developed by

Received 14 February 1994; revised 28 July 1994; accepted 22 September 1994

Hill and Karlsson[7,8] expresses load dynamics in terms of aggregate static and transient load characteristics. In Reference 7, it is shown that this general nonlinear model captures the dynamical behaviour of various loads including motors, tap-changers, static loads and thermostat controlled resistive devices. This was subsequently used to explore static vs. dynamic aspects of voltage stability. In Reference 7 the single line case was studied; results for the general case are presented in References 11 and 16.

This paper investigates the nature of voltage collapse by modelling the dynamics of aggregate loads and voltage control equipment such as transformer tap-changers, and examining the dynamic interaction between them. In Reference 5, 'leaf' diagrams were proposed as a way of explaining this interaction and revealing a mechanism of voltage collapse. As for the control action, it was shown that locking the tap changers at an appropriate time which corresponded to voltage recovery helped the system voltage to reach a steady-state, and therefore avoid the collapse. These results were obtained using load dynamics with an instantaneous recovery to a steady-state level. We show that with a more realistic (exponential) recovery produced by a general nonlinear recovery load model[7], the earlier conclusions regarding tap locking do not always hold true. Besides that, the important issue of the 'timing' of tap locking is particularly investigated. It is shown that in most cases the tap locking problem can be analysed as a bifurcation problem. The latest appropriate time to perform the tap locking corresponds to a bifurcation point of the system model. Some special situations where this does not hold true are addressed.

The structure of the paper is as follows. Section II develops a model for single-line single-load power systems which incorporates tap changer dynamics and dynamic load with exponential recovery. Section III presents leaf diagrams, and briefly reviews the main results of the voltage stability analysis presented in References 3 and 5, which corresponded to the use of non-recovery load modelling. Insights into the mechanism of voltage collapse when load recovery is modelled are revealed in Section IV. The voltage collapse phenomenon in a simple power system is analysed by examining the dynamic interaction between the load and its supply network. From this analysis, the use of tap locking as a way of preserving load voltage is investigated. Detailed information on the determination of the latest time to lock taps, along with some supporting simulation results, are presented in Section V. Conclusions are given in Section VI. Further details are available in Reference 15.

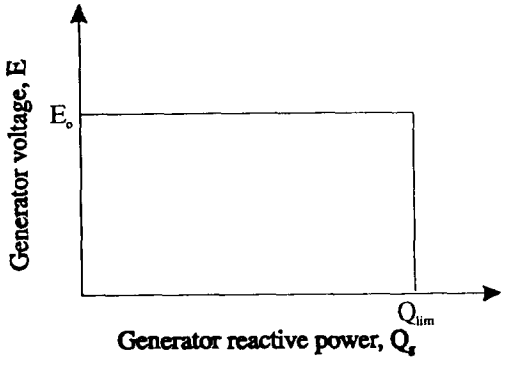

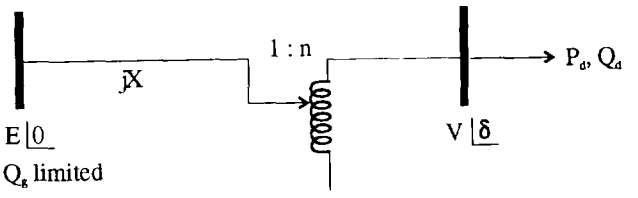

Figure 1. A two-node system

II. System model

A general model for the study of the interaction between generator limits, tap-changing transformers and load dynamics is developed in References 15 and 16. In this paper we concentrate on the simple power system shown in Figure 1. Therefore, the reduced model applicable to this simple power system will be outlined here.

In this simple power system, we have only one generator bus. We shall therefore take that bus as the reference bus, i.e., the voltage angle is set to zero. Also, swing dynamics are not a consideration. The generator terminal voltage is denoted by E. Its reactive output Q_g has an upper limit of $Q_{\lim}$. The terminal voltage and reactive power have the following characteristic:
This characteristic can be described by,

$$E = E_0 \quad \text{if} \quad Q_g(E_0) \leqslant Q_{\lim}$$

$$Q_g(E) = Q_{\lim} \quad \text{if} \quad Q_g(E_0) > Q_{\lim}$$

Note that at the point where the limit is first encountered, both the above constraints (on E and Q_g) are satisfied.

For simplicity, assume the system is lossless, i.e., the impedance of the transmission line is jX. Let the turns ratio of the transformer be n, and let P_l, Q_l denote the total real and reactive power entering the load bus via the transformer. Then

$$P_l(\delta, V, E, n) = -\frac{EV}{nX}\sin\delta \tag{1}$$

$$Q_l(\delta, V, E, n) = -\frac{V^2}{n^2X} + \frac{EV}{nX}\cos\delta \tag{2}$$

Now consider the modelling of the load. Measurements in the laboratory and on power system buses show that a typical load response to a step in voltage V is of the form shown in Figure 2 for reactive power Q_d, and similarly for real power[8]. It can be seen that a sudden voltage step causes an instantaneous power demand step ΔQ_t. This step defines the transient characteristics $Q_t(V)$ of the load. Following this the demand recovers to a steady-state value. The steady-state power demand is a function of the steady-state voltage and this function defines the steady-state load characteristics $Q_s(V)$. The time constant for a load to recover to steady-state is denoted as T_q. Based on this form of response, Reference 7 proposes a nonlinear recovery model which captures such load behaviour. Considering reactive power, the model can take the form of a scalar differential equation

$$T_q\dot{Q}_d + Q_d = Q_s(V) + k_q(V)V \tag{3}$$

or first-order normal form

$$\dot{x}_q = -T_q^{-1}x_q + N_q(V) \tag{4}$$

$$Q_d = T_q^{-1}x_q + Q_t(V) \tag{5}$$

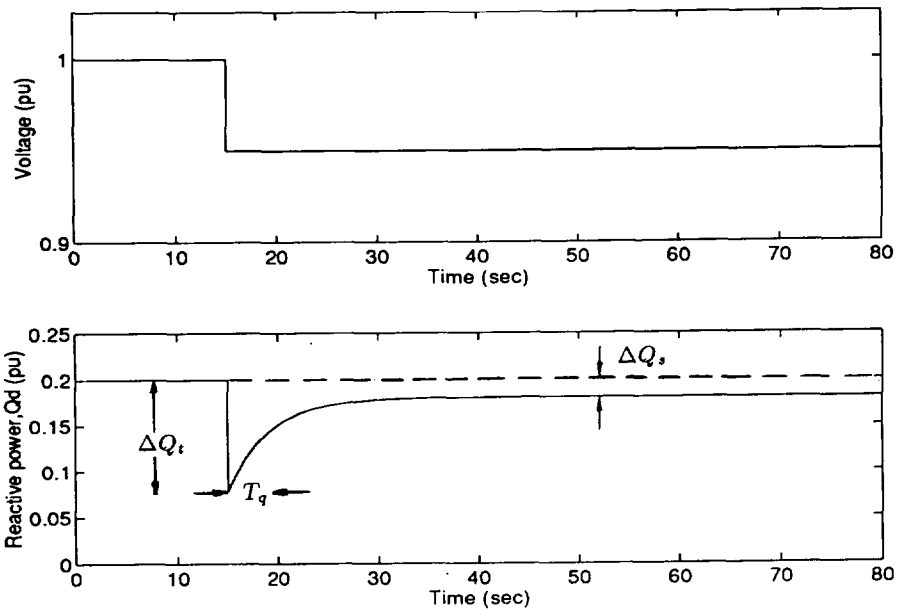

Figure 2. Recovery load response to a step voltage change

where

$$\frac{dQ_t}{dV} = T_q^{-1} k_q(V) \tag{6}$$

$$N_q(V) = Q_s(V) - Q_t(V) \tag{7}$$

Similar equations hold for real power P_d related to V.

This approach to load modelling is flexible enough to study various time-scales corresponding to induction motor, tap-changer or thermostat control transient behaviour.[7]

The functions Q_s and Q_t (and likewise P_s and P_t) can take various forms. One simple choice is the usual single index form

$$Q_s(V) = Q_s^0 V^{\beta_s} \tag{8}$$

$$Q_t(V) = Q_t^0 V^{\beta_t} \tag{9}$$

which separates static and transient behaviour by using indices β_s and β_t respectively. In the analysis of voltage collapse, other models for static characteristics are sometimes preferred, e.g.,

$$Q_s(V) = b_0 + b_1 V + b_2 V^{\beta_s} \tag{10}$$

Depending on the nature of the real and reactive power loads, we define

$$\begin{aligned} 0 &= P_d - T_p^{-1} x_p - P_t(V) \\ &:= g_1(V, x_p, P_d) \quad \text{for dynamic } P_d \\ 0 &= P_d - P_d(V) \\ &:= g_1(V, x_p, P_d) \quad \text{for static } P_d \end{aligned} \tag{11}$$

and

$$\begin{aligned} 0 &= Q_d - T_q^{-1} x_q - Q_t(V) \\ &:= g_3(V, x_q, Q_d) \quad \text{for dynamic } Q_d \\ 0 &= Q_d - Q_d(V) \\ &:= g_3(V, x_q, Q_q) \quad \text{for static } Q_d \end{aligned} \tag{12}$$

Note that functions $P_d(V)$, $Q_d(V)$ could be constant or in fact zero.

Consider the modelling of the tap-changer. Tap-changers are a special type of transformer whose turns-ratio is automatically adjusted in order to regulate the voltage of a specified bus, i.e., usually the voltage at the secondary side of the transformer. The tap-changer has a reference voltage value V^0, which is the target value of an automatic voltage regulator. The tap movements are discrete and can be modelled by

$$n(t) = n(t^-) - df(V - V^0) \tag{13}$$

where $d \in R^+$ is the size of each tap-step,

$$f(x) = \begin{cases} -1 & \text{if } x \leqslant -\epsilon \\ 0 & \text{if } |x| < \epsilon \\ 1 & \text{if } x \geqslant \epsilon \end{cases} \tag{14}$$

and $(-\epsilon, \epsilon)$ is the deadband[10]. An alternative to (13) is a continuous-time model of tap changing. This model could be written as,

$$\frac{dn}{dt} = \frac{1}{T}(V^0 - V) \tag{15}$$

where T is the tapping time constant of the transformer. This model provides an acceptable approximation of discrete tap movements over the longer term and so forms a convenient basis for the analytical study of voltage collapse behaviour.

Combining the transformer tap dynamic equation (15) with the equations describing the power balance at the load bus, which are derived from (1)–(12), gives the total system representation

$$\dot{n} = T^{-1}(V^0 - V) \qquad := f_1(V) \tag{16}$$

$$\dot{x}_p = -T_p^{-1} x_p + N_p(V) \qquad := f_2(x_p, V) \tag{17}$$

$$\dot{x}_q = -T_q^{-1} x_q + N_q(V) \qquad := f_3(x_q, V) \tag{18}$$

$$0 = g_1(V, x_p, P_d) \tag{19}$$

$$0 = -P_l(\delta, V, E, n) + P_d \qquad := g_2(\delta, V, E, n, P_d) \tag{20}$$

$$0 = g_3(V, x_q, Q_d) \tag{21}$$

$$0 = -Q_l(\delta, V, E, n) + Q_d \qquad := g_4(\delta, V, E, n, Q_d) \tag{22}$$

This model is a set of differential-algebraic (DA)

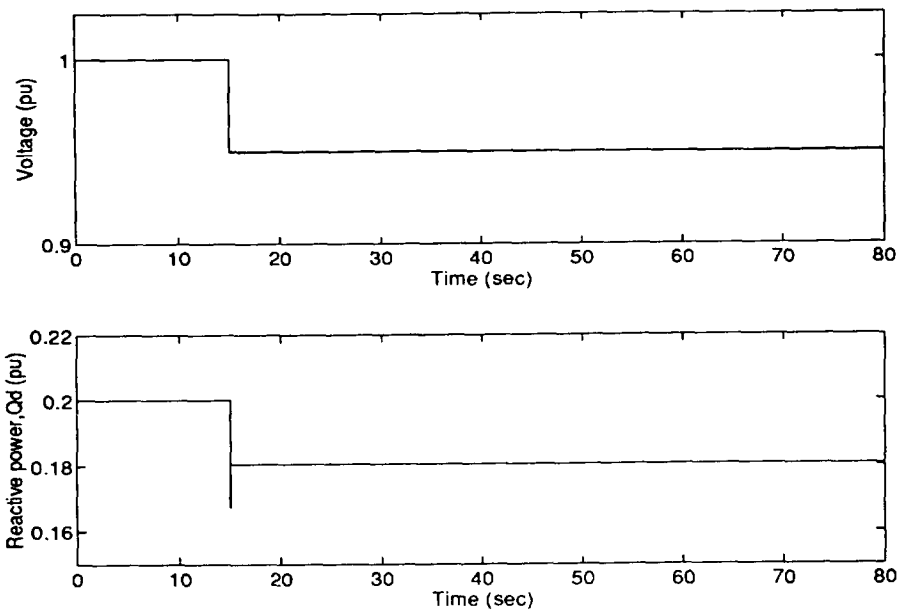

Figure 3. Non-recovery load response to a step voltage change

equations. The dynamic states of the system are the tap position n and load dynamic variables x_p and x_q, whilst the algebraic variables are bus quantities δ, V, P_d and Q_d. Define $g = [g_1\, g_2\, g_3\, g_4]^t$. Then $g(n, x_p, x_q, \delta, V, P_d, Q_d) = 0$ defines a 3-manifold called the constraint manifold. The system always remains on that manifold and is driven over it by the dynamics of (16)–(18).

The model (16)–(22) assumes that the generator voltage is fixed at E_0, so that the reactive power equation at the generator bus is deleted. But, if the generator reactive power Q_g becomes fixed (at its limit), the generator voltage E becomes a variable, and a reactive power equation at the generator bus given by

$$0 = Q_g(\delta, V, E, n) - Q_{\lim} \quad := g_5(\delta, V, E, n) \tag{23}$$

should be added to the system model (16)–(22). Then, the constraint manifold will be augmented by equation g_5, and will involve one more variable, the generator terminal voltage E. The constraint manifold will remain of dimension 3.

As mentioned earlier, the extension of the above simple system model to a multimachine multiload system model is given in References 15 and 16.

III. Voltage collapse with non-recovery load model

The load modelling approach given by (4)–(7) provides separate nonlinear static and transient behaviour defined by load functions $P_s(V)$ and $P_t(V)$, and/or $Q_s(V)$ and $Q_t(V)$. Setting recovery time constants $T_p = T_q = 0$ gives that the response of an aggregate load to the voltage step is of the form shown in Figure 3 for reactive power Q_d, and similarly for real power P_d. As with the recovery model, a sudden voltage change causes an instantaneous power demand change. But following this the demand recovers instantaneously to a steady-state level. This model is used in References 3 and 5 for analysing the dynamic process of voltage collapse based on the interaction of tap changer dynamics, load dynamics and generation limits. In Reference 5, 'leaf' diagrams were proposed as a way of explaining this interaction. A simple power system of Figure 1 is analysed. For this system, a region in the state space which corresponds to the recovery of voltage is identified. This region is conveniently visualized in terms of load voltage and tap position. This voltage recovery ($\dot{V} > 0$) region, which was referred to as the 'leaf', is enclosed within the curve defined by $\dot{V} = 0$. Manipulation of the model equations obtained from setting $\dot{V} = 0$ results in the analytical expression for the region boundary,

$$[P_s^2(V) + Q_s^2(V)]n^4 + \left[2Q_s(V) - \frac{E^2}{X}\right]\frac{V^2}{X}n^2 + \frac{V^4}{X^2} = 0 \tag{24}$$

Two versions of the region boundary are shown in Figure 4. Curve 1 was obtained by setting $E = E_0$. However, at a large number of points in curve 1, the reactive power limit of the generator was exceeded, i.e., $Q_g(E_0) > Q_{\lim}$. Curve 2 shows the restriction of the region boundary obtained by taking into account the generator operation at the limit. Where the curves do not overlap, the value of E, which satisfies $Q_g(E) = Q_{\lim}$, is less than E_0. Because of that the region $\dot{V} > 0$ becomes significantly smaller. The equilibrium points are given by the intersection of the region boundary with a line corresponding to the set point voltage V^0, as shown in Figure 4. The shape of the region $\dot{V} > 0$ depends on the load models for P_s and Q_s; the particular shape given in Figure 4 arises when P_s is set to zero and Q_s is a quadratic function of V. As long as the system trajectory is inside the recovery region, the load voltage recovers. In References 3 and 5, a different approach was taken in handling the generator reactive power limit. Rather than explicitly determining the restriction to the recovery region caused by the generator limit (and given in Figure 4 by curve 2), the idea of shrinking leaves was proposed. After the generator limit is encountered, E begins to fall from the setpoint value E_0. For each reduced value of E, a new leaf is defined by (24). It was shown that as E reduces, a succession of smaller and smaller leaves, each one contained completely within the previous one, is obtained. (Note though that only one point on each of these leaves will satisfy $Q_g = Q_{\lim}$. That

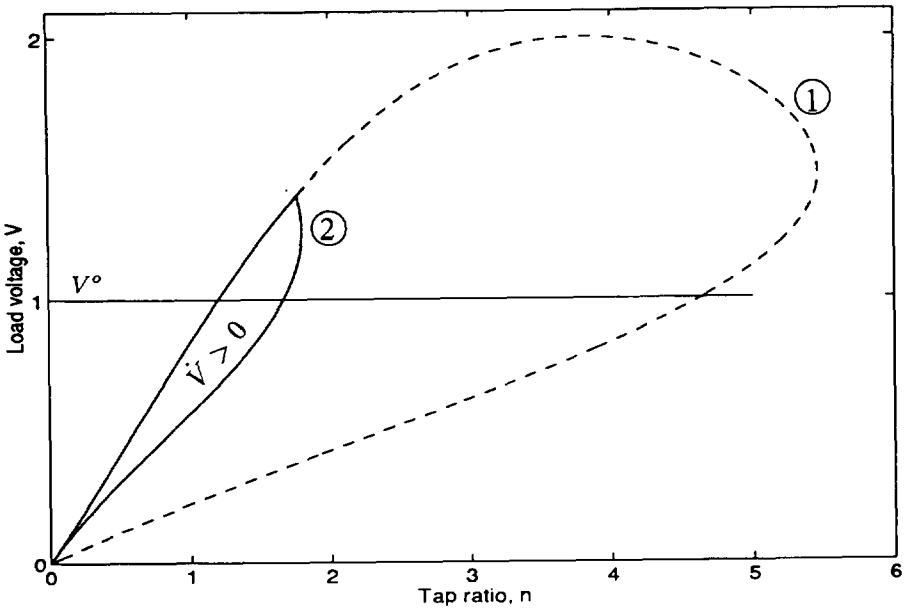

Figure 4. Leaf diagram in the $n-V$ plane

point would occur at the intersection of the contracted leaf and the right section of curve 2.) Voltage collapse can occur by either the system trajectory moving outside the leaf, or the leaf contracting from around the system trajectory. In both cases, the point at which the system exits the leaf must satisfy $\dot{V} = 0$. It must therefore correspond to a point on curve 2 of Figure 4. If at the exit point $E < E_0$, then by definition $Q_g = Q_{\lim}$. In that case it will correspond to a point on the right section of curve 2.

Based on such dynamic considerations, it was also found that it is possible to avoid voltage collapse if the tap changer is locked while the system trajectory is inside the recovery region. For a physical view, note that when the voltage is recovering (trajectory is inside the recovery region) the continuing action of the tap changer may further reduce the receiving-end voltage of the transmission line V/n due to an increasing n. If one decides to lock the tap while the trajectory is inside the recovery region, then V/n will improve since V increases and n is fixed. This implies that the reactive loss due to the transmission line can be reduced and the burden on the generator is lessened. The generator terminal voltage E can recover and hence, in the shrinking leaf view, the leaf expands. The system trajectory continues moving vertically upward (n fixed) and approaches the boundary of the recovery region where $V = 0$. The load voltage settles to a steady-state value. However, it may be lower than the reference voltage V^0. The effect of this tap locking strategy is illustrated in Figure 5[5].

IV. Voltage collapse with recovery load model

IV.1 *Features of the single-line system*

In Section III it was stated that if load is modelled with no

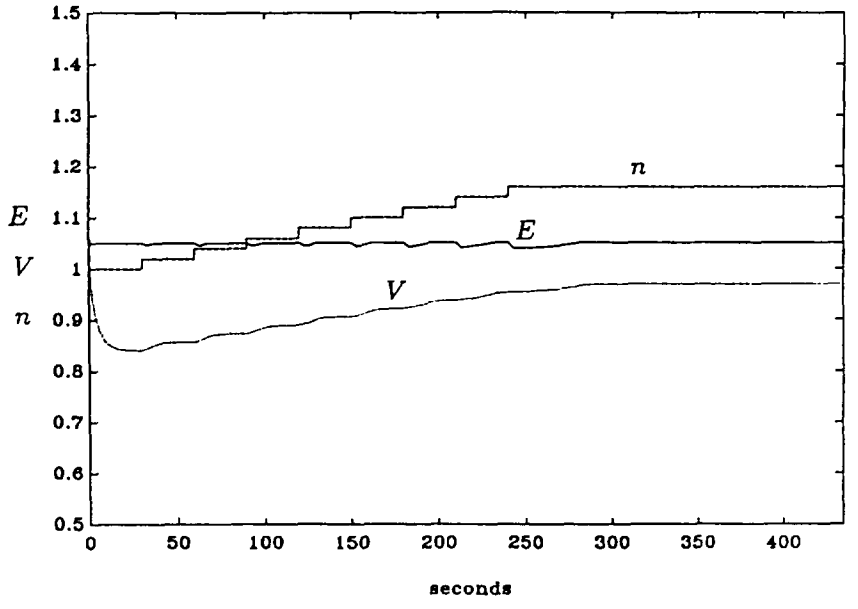

Figure 5. Voltage recovery by tap locking

recovery mechanism, then voltage collapse can be avoided if the locking takes place when the system trajectory, which in that case is driven by voltage dynamics, is inside the leaf. The use of a more general, nonlinear recovery load model given by (3) provides novel insights into the mechanism of voltage collapse. The extra dynamic terms $T_p\dot{P}_d$ and/or $T_q\dot{Q}_d$ make a major difference regarding the decision when to lock the tap changer to prevent a voltage collapse arising.

To illustrate some properties of this model, the single load system of Figure 1 is explored in this section. Dynamic behaviour of the load model is most clearly illustrated when only the real power load or reactive power load is modelled dynamically, with the other being modelled by some static voltage characteristic. Assume that reactive load is modelled by (3), and for convenience the real load is set to zero. Since $P_d = 0$, equations (1) and (20) give $\delta = 0$ everywhere and Q_l only depends on V and n. From equations (7), (16), (18), (21) and (22) the system is described by the differential-algebraic set of equations

$$\dot{n} = T^{-1}(V^\circ - V) \tag{25}$$

$$\dot{x}_q = -T_q^{-1}x_q + Q_s(V) - Q_l(V) \tag{26}$$

$$0 = -Q_l(V,n) + T_q^{-1}x_q Q_l(V) \tag{27}$$

It is useful to note that (26) has an equivalent convenient form. Combining (26) and (27) gives

$$\dot{x}_q = Q_s(V) - Q_l(V,n) \tag{28}$$

which means that the load dynamics is driven by the reactive power mismatch. Setting derivative $\dot{x}_q$ to zero gives the static model $Q_s(V) = Q_l(V,n)$, which is the same as the static model in Section III obtained by setting $\dot{V} = 0$. It means that it represents the same curve in the n–V plane as is shown in Figure 4. But now, the region $\dot{x}_q < 0$ is enclosed within the curve defined by (24) where $P_s(V)$ is set to zero (since we assume $P_d = 0$). It is no longer appropriate to call this region the voltage recovery region. However we see from (28) that $\dot{x}_q < 0$ corresponds to $Q_l(V,n) > Q_s(V)$, i.e., the load demand is greater than the steady-state load requirement. We shall therefore refer to this region as the (transient) excess load region.

The equilibria of the system are intersections of the curves $V = V^\circ$ and the boundary of the excess load region, $\dot{x}_q = 0$. From (27),

$$x_q = T_q(Q_l(V,n) - Q_l(V)) \tag{29}$$

so the corresponding curve in the n–x_q plane is given in Figure 6 where

$$x_q^\circ = T_q(Q_s(V^\circ) - Q_l(V^\circ)) = T_q N_q(V^\circ) \tag{30}$$

Again, curve 1 represents the boundary of the region obtained for $E = E_0$, whilst curve 2 takes into account generator operation at its limit, in which case the actual E is less than E_0. The dotted line denoted by $Q_{\lim}$ gives points where the generator makes the transition between regulating E and being limited, or vice versa, i.e., points which satisfy both (23) and $E = E_0$. So for the system in Figure 1, the generator terminal voltage E is given by

$$E = \min\left\{E_0, \sqrt{Q_{\lim}X + \frac{V^2}{2n^2} + \frac{1}{2}\sqrt{\frac{V^4}{n^4} + 4\frac{V^2}{n^2}XQ_{\lim}}}\right\} \tag{31}$$

where the second term in the minimization refers to (23), i.e., generator operation at its reactive power limit. As seen, the effect of the generator reactive limit is to contract the $\dot{x}_q < 0$ region. It will be shown in the sequel that this contracted excess load region plays an important role in the mechanism of voltage collapse.

It is useful to supplement the view of the excess load region in the n–V and n–x_q planes, shown in Figures 4 and 6, by the corresponding view in the V–x_q plane. It follows from (26) that the curve given by

$$x_q = T_q(Q_s(V) - Q_l(V)) \tag{32}$$

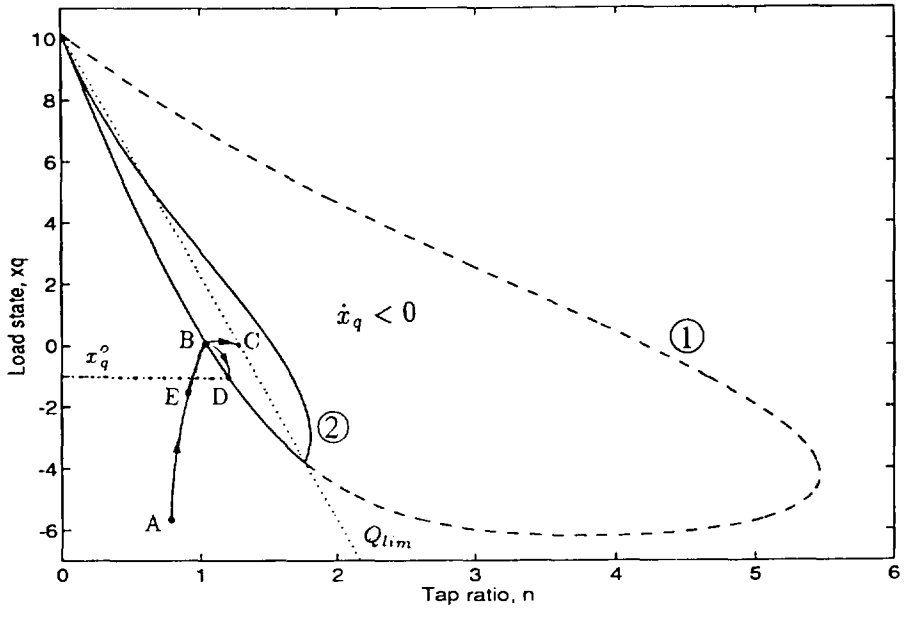

Figure 6. Excess load region as viewed in the n–x_q plane

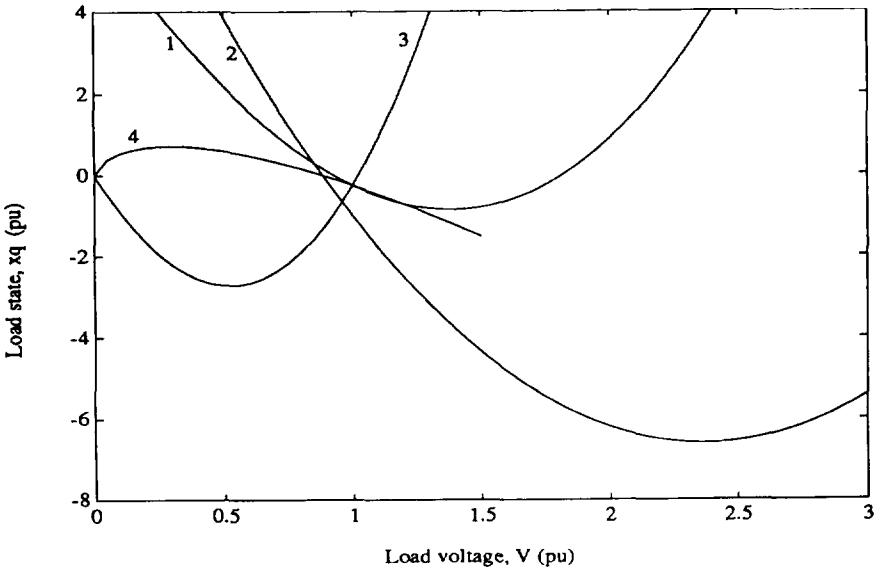

Figure 7. Boundary of the excess load region as viewed in the $V-x_q$ plane for various reactive static characteristics:
(1) $Q_s(V) = 0.4 + 0.1V + 0.15V^{2.4}$ (3) $Q_s(V) = 0.65V^{2.1}$
(2) $Q_s(V) = 0.68 - 0.28V + 0.2V^2$ (4) $Q_s(V) = 0.65V^{0.8}$

defines all points where $\dot{x}_q = 0$. Notice that the shape of this curve depends only on the static and transient load characteristics. Some possible shapes for this curve, as viewed in the $V - x_q$ plane, are shown in Figure 7. In producing these curves, $Q_t(V)$ was specified as a linear function of V, i.e., $Q_t(V) = (k_q/T_q)V$, where $K_q = 10$, $T_q = 15$ s. The parameters of $Q_s(V)$ were varied. As can be seen, the general shape of all these curves is almost the same, except the one shown by curve 4. The difference is a consequence of the fact that in this case the $Q_t(V)$ characteristic has a greater voltage exponent than the $Q_s(V)$ characteristic, which results in a maximum as an extreme point. As in the case of the excess load region shown in Figures 4 and 6, $\dot{x}_q < 0$ at all points inside the region, i.e., above the curve, and $\dot{x}_q > 0$ at all points outside the region, i.e., below the curve. These curves will be used in the analysis in Section V, where tap locking strategies which alleviate voltage collapse will be explored.

It is interesting to note that static characteristic 3 differs from the others in terms of its effect on singularity of the Jacobian of the equations which describe the $\dot{x}_q = 0$ curve. From (26), (27), it can be seen that $\dot{x}_q = 0$ corresponds to $0 = -Q_l(V,n) + Q_s(V)$. In Reference 14, it was conjectured that if the voltage index β_s was greater than 1, singularity of the Jacobian would not occur. For indices less than 1, singularity was a possibility. Only characteristic 3 satisfies that criteria for Jacobian non-singularity. (Characteristics 1 and 2 fail due to their constant power terms.) As a consequence, the $\dot{x}_q = 0$ curves for characteristics 1, 2 and 4 are always bounded in the direction of increasing n. Figures 8 and 11 provide examples. For characteristic 3, such curves are unbounded in the n direction, see Figure 10.

The power system of Figure 1 is used in the sequel to illustrate voltage collapse scenarios, and later tap locking strategies. The following parameters of this system have been used in all cases:

$$E_0 = 1.05\,\text{p.u.}, X = 0.3\,\text{p.u.}, V^o = 1\,\text{p.u.},$$
$$T = 62\,\text{s}, k_q = 10, T_q = 15\,\text{s}$$

Various static reactive power load characteristics have been used for different cases. Also, the value of the generator reactive power limit varies between cases. Details of those parameters are provided as appropriate.

IV.2 *Voltage collapse analysis*

Having established some general properties of the load state behaviour, we now consider how a voltage collapse arises from the interaction of the load dynamics described by the nonlinear recovery model, tap changing, and generator reactive capability limiting.

Referring to Figure 6, assume that the system has been operating in a steady state point A when a disturbance occurs, such as an increase in loading. The operating point A is outside the post-disturbance $\dot{x}_q < 0$ region, and because of that, the x_q trajectory is moving up (i.e., $\dot{x}_q > 0$). At point B, the x_q trajectory enters the excess load region and changes direction, i.e., begins to move down. If the trajectory does not cross the generation limit curve Q_{lim}, then it would trace a path from point B to point D within the excess load region. If, on the other hand, this trajectory crosses the limit curve at some point C, the generator will operate at its limit and its terminal voltage decreases. The part of the region where $E < E_0$, i.e., curve 2, is now relevant, so the x_q trajectory may soon fall outside the $\dot{x}_q < 0$ region. It is then moving up. As will be shown in the sequel, during that time $V < V^o$, so that the tap ratio steadily increases. It means that the x_q trajectory is moving up but away from the boundary $\dot{x}_q = 0$. Voltage collapse takes place.

Note that the voltage collapse may not always happen in this way. Depending on load parameters, the relative positions of the curves corresponding to tap changer dynamics, load dynamics and generation limit may change, and the sequence of events may be different. This will be described and illustrated after the following analytical discussion of the voltage collapse scenario.

If follows from (29) that voltage dynamics are given by

$$\dot{V} = -T_q^{-1} \frac{1}{\dfrac{\partial(Q_t - Q_l)}{\partial V}} \dot{x}_q - \frac{\dfrac{\partial(Q_t - Q_l)}{\partial n}}{\dfrac{\partial(Q_t - Q_l)}{\partial V}} \dot{n} \tag{33}$$

Considering a very small time interval, tap ratio variation is typically much slower than variation of $x_q (T \gg T_q)$. It means that for small movement away from point A, with x_q increasing, the tap ratio can be assumed unchanged. The change in load voltage V in response to the increase in x_q is then given by

$$\Delta V \simeq -T_q^{-1} \frac{1}{\dfrac{\partial(Q_t - Q_l)}{\partial V}} \Delta x_q \tag{34}$$

Assume that $Q_t(V)$ is a linear function of V, i.e., $Q_t(V) = (k_q/T_q)V$, where $k_q > 0$, $T_q > 0$. Then, $[\partial Q_t(V)]/\partial V$ at point A is positive. It is shown in the Appendix that under normal conditions $[\partial Q_l(V,n)]/\partial V$ for the post-fault system characteristic is negative. Therefore, an increase in x_q results in a decrease in V. But, according to (25) a decrease in V will provoke an increase in n. The $\dot{n}$ term of (33) will begin to become significant. Again, from the Appendix, under normal conditions $[\partial Q_l(V,n)]/\partial n$ will be positive. Because of that, the rate of downward movement in voltage is decreasing and at one moment $\dot{V}$ becomes zero (point E in Figure 6). Since at that point the $\dot{x}_q = 0$ curve has not been encountered, $\dot{x}_q$ remains positive; x_q trajectory continues moving up and load voltage starts to increase but is still $V < V^\circ$ which means that n continues to increase. In this scenario, after time the system will reach a point where $\dot{x}_q = 0$ (point B in Figure 6). From (28) it can be seen that at that point, $Q_l(V,n) = Q_s(V)$. Voltage dynamics are given by

$$\dot{V} = -\frac{\dfrac{\partial(Q_t - Q_l)}{\partial n}}{\dfrac{\partial(Q_t - Q_l)}{\partial V}} \dot{n} = \frac{\dfrac{\partial Q_l}{\partial n}}{\dfrac{\partial(Q_t - Q_l)}{\partial V}} \dot{n} \tag{35}$$

Since $\partial Q_l/\partial n$, $[\partial(Q_t - Q_l)]/\partial V$ and $\dot{n}$ are still positive at point B, $\dot{V}$ will remain positive too. At point B, $\dot{x}_q$ changes from being positive to being negative, so the trajectory begins to decline. Because $\dot{x}_q < 0$, (33) implies that generally V will continue to increase until the boundary $\dot{x}_q = 0$ is touched again (point D) and $\dot{n}$ becomes zero. The system will settle at $V = V^\circ$, i.e., $x_q = x_q^\circ$.

This analysis has shown that if the trajectory doesn't cross the limit curve $Q_{\lim}$, voltage recovery will occur on the path E–B–D. We now wish to consider the case when the trajectory crosses the limit curve. The generator is then at its limit and its voltage is given by the second term in (31). From (29), (31), voltage dynamics are then given by

$$\dot{V} = -T_q^{-1} \frac{1}{\dfrac{\partial(Q_t - Q_l)}{\partial V} - \dfrac{\partial Q_l}{\partial E}\dfrac{\partial E}{\partial V}} \dot{x}_q - \frac{\dfrac{\partial(Q_t - Q_l)}{\partial n} - \dfrac{\partial Q_l}{\partial E}\dfrac{\partial E}{\partial n}}{\dfrac{\partial(Q_t - Q_l)}{\partial V} - \dfrac{\partial Q_l}{\partial E}\dfrac{\partial E}{\partial V}} \dot{n} \tag{36}$$

Assume that the trajectory is outside the excess load region (i.e., it is moving upward), and crosses the $Q_{\lim}$ curve while load voltage is recovering (path E–B in Figure 6). The generator is now at its limit and its voltage E starts to decrease. Since $[\partial(Q_t - Q_l)]/\partial V$, $\partial Q_l/\partial E$, $\partial E/\partial V$, $\partial Q_l/\partial n$ are positive, and $\partial E/\partial n$ is negative (see Appendix), the detailed analysis of the terms in (36) given in the Appendix shows that at the point as E starts to decrease and $V < V^\circ$ both

$$\left[\frac{\partial(Q_t - Q_l)}{\partial V} - \frac{\partial Q_l}{\partial E}\frac{\partial E}{\partial V}\right] \text{ and } \left[\frac{\partial(Q_t - Q_l)}{\partial n} - \frac{\partial Q_l}{\partial E}\frac{\partial E}{\partial n}\right]$$

can be regarded as positive. Because of that, it follows from (36) that $\dot{V}$ becomes negative and voltage decreases. The rate of the tap ratio movement is increased. There are two possibilities.

- If load and generator voltages decrease rapidly, $\dot{x}_q > 0$

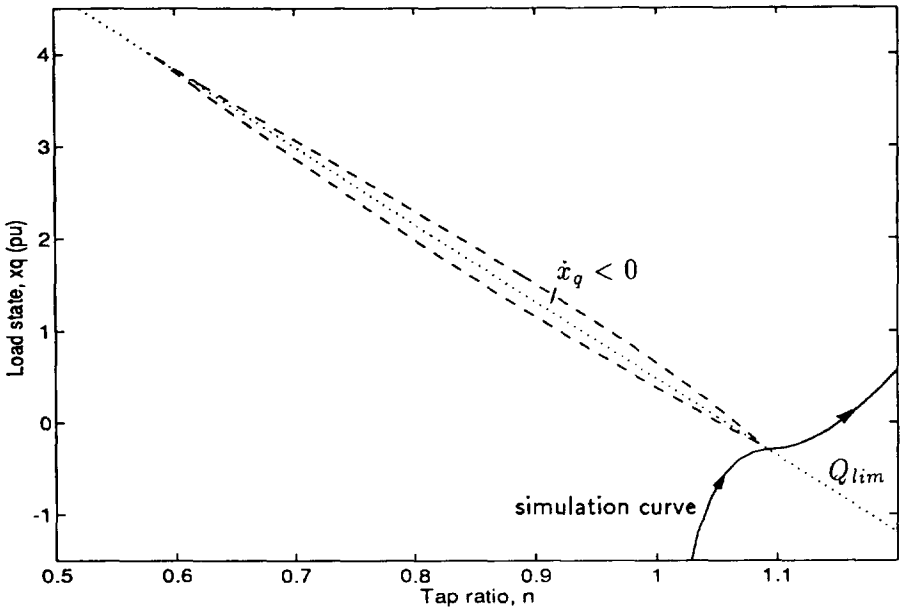

Figure 8. Excess load region and voltage collapse scenario as viewed in the n–x_q plane; $Q_s(V) = 0.68 - 0.28V + 0.2V^2$, $Q_{\lim} = 0.74$

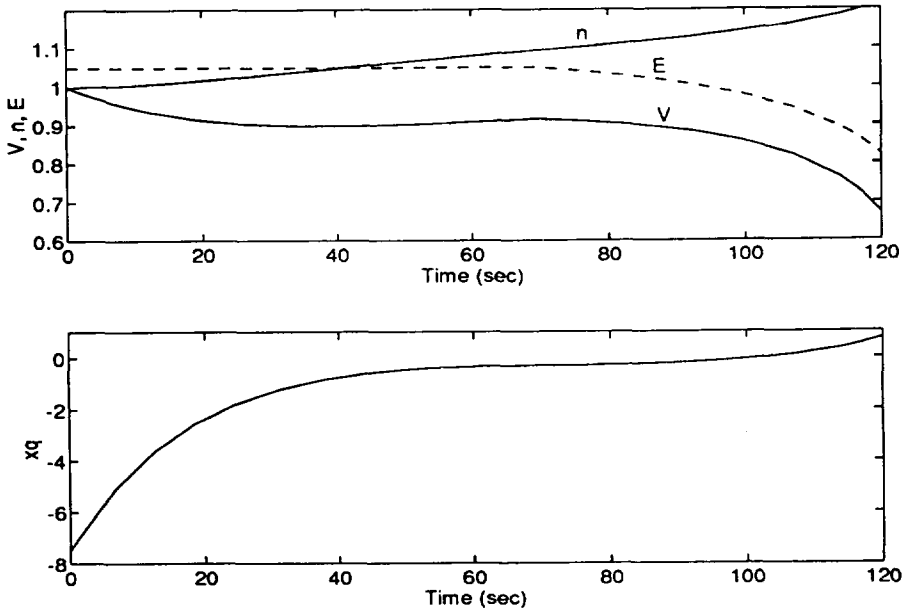

Figure 9. Voltage collapse scenario in time domain: $Q_s(V) = 0.68 - 0.28V + 0.2V^2$, $Q_{\text{lim}} = 0.74$

will start to increase, i.e., upward movement can become faster, but the generator will continue to work on its limit. So, the load voltage continuously decreases, i.e., the tap ratio steadily increases and the system trajectory is moving up but far away from the boundary $\dot{x}_q = 0$. This case is illustrated in Figure 8 where the system trajectory is presented in the n–x_q plane along with the corresponding contracted excess load region (denoted by dashed lines in Figure 8). The equivalent representation in the time domain is shown in Figure 9.

- If load voltage decreases slowly, then it is possible that the trajectory may enter the $\dot{x}_q < 0$ region. This will not change the voltage direction, i.e., it will continue decreasing. This will lead to a further reduction of generator voltage and increase of tap ratio. As a result, the system trajectory may soon fall outside the $\dot{x}_q < 0$ region again. It will then again move up toward the boundary $\dot{x}_q = 0$. But, in the scenario illustrated in Figure 10, it cannot reach the boundary and voltage collapse takes place.

Voltage collapse can also happen when the trajectory is inside the $\dot{x}_q < 0$ region and crosses the Q_{lim} curve (point C in Figure 6). As mentioned above,

$$\left[\frac{\partial(Q_t - Q_l)}{\partial V} - \frac{\partial Q_l}{\partial E}\frac{\partial E}{\partial V}\right] \text{ and } \left[\frac{\partial(Q_t - Q_l)}{\partial n} - \frac{\partial Q_l}{\partial E}\frac{\partial E}{\partial n}\right]$$

are positive at that moment, so from (36), $\dot{V}$ changes sign, i.e., load voltage starts to decrease which provokes faster increasing of tap ratio and decreasing of generator voltage. As a result, the trajectory can fall outside the $\dot{x}_q < 0$ region, and begin to move up again. Owing to further increasing of tap ratio, it will move away from the

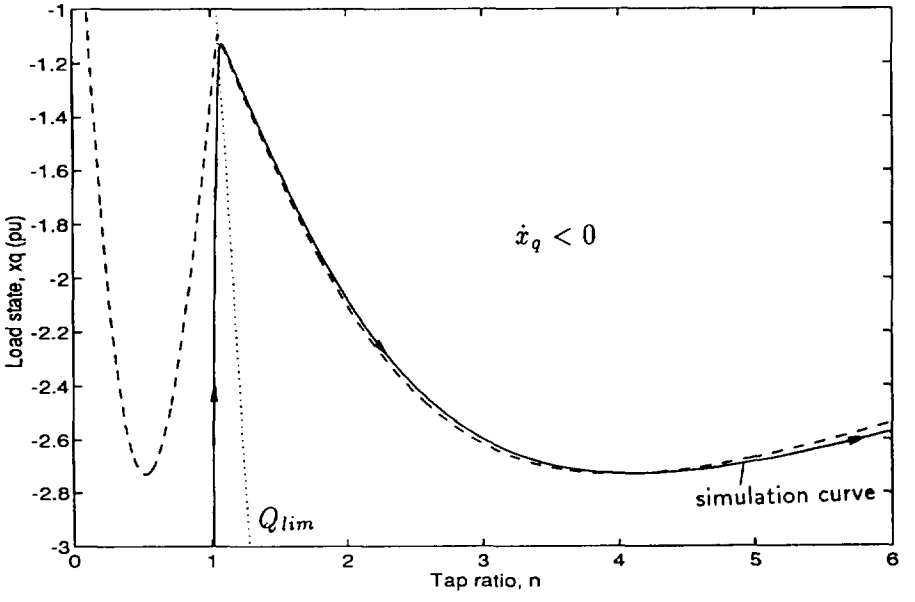

Figure 10. Excess load region and voltage collapse scenario as viewed in the n–x_q plane; $Q_s(V) = 0.65V^{2.1}$, $Q_{\text{lim}} = 0.65$

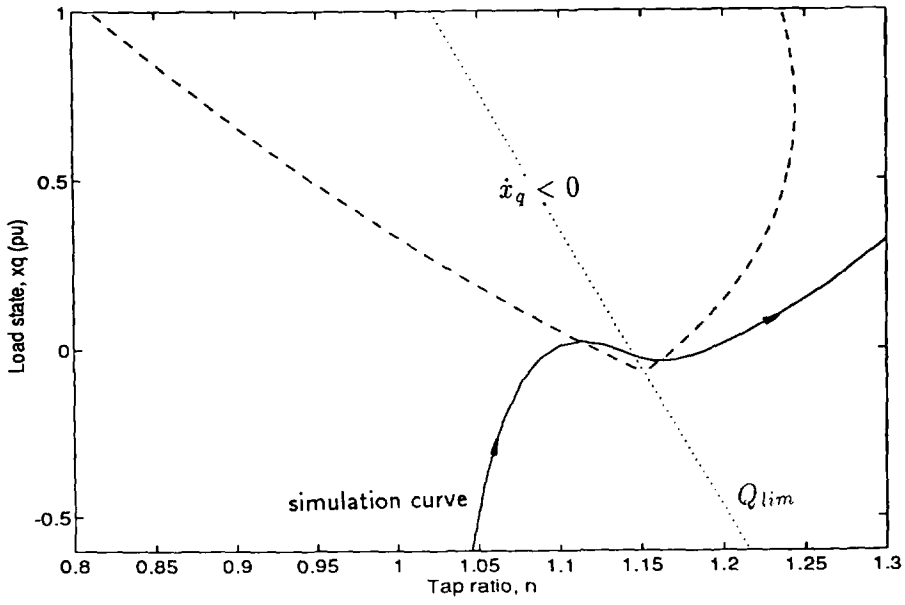

Figure 11. Excess load region and voltage collapse scenario as viewed in the n–x_q plane; $Q_s(V) = 0.4 + 0.1V + 0.15V^{2.4}$, $Q_{lim} = 0.8$

$\dot{x}_q = 0$ boundary as is illustrated in Figure 11. Load voltage continuously decreases and voltage collapse takes place.

Note that in these voltage collapse scenarios, the system trajectory either exits (Figures 10 and 11) or passes by (Figure 8) the $\dot{x}_q < 0$ region from its low side, i.e., from under the $\dot{x}_q = 0$ curve. For the purpose of the later analysis of control action, it is useful to show one more possible voltage collapse scenario. Figure 12 illustrates the case where the trajectory exits the $\dot{x}_q < 0$ region from its upper side. The importance of such system trajectory behaviour during voltage collapse will be emphasized in the next section where the problem of timing of tap changer control is explored.

Another way of illustrating the voltage collapse scenario is to consider the constraint manifold described by (27), including the effect of generator capability limit given by (31). This surface is shown in Figure 13 in the space of (V, n, x_q). One projection of this surface is shown in Figure 14. In this view the surface is composed of contours, each one of which corresponds to a different constant n. The corresponding $\dot{x}_q = 0$ curve (from Figure 7), the line corresponding to $\dot{n} = 0$, and the simulation of Figure 8 (or 9) as viewed in the V–x_q plane are added to illustrate the voltage collapse scenario. Note that the fold in the surface corresponds to the generator encountering its limit. It is easy to see that the trajectory never enters the $\dot{x}_q < 0$ region. As n and x_q increase, it crosses the fold in the surface before it gets to the boundary of that region. Consequently, after the

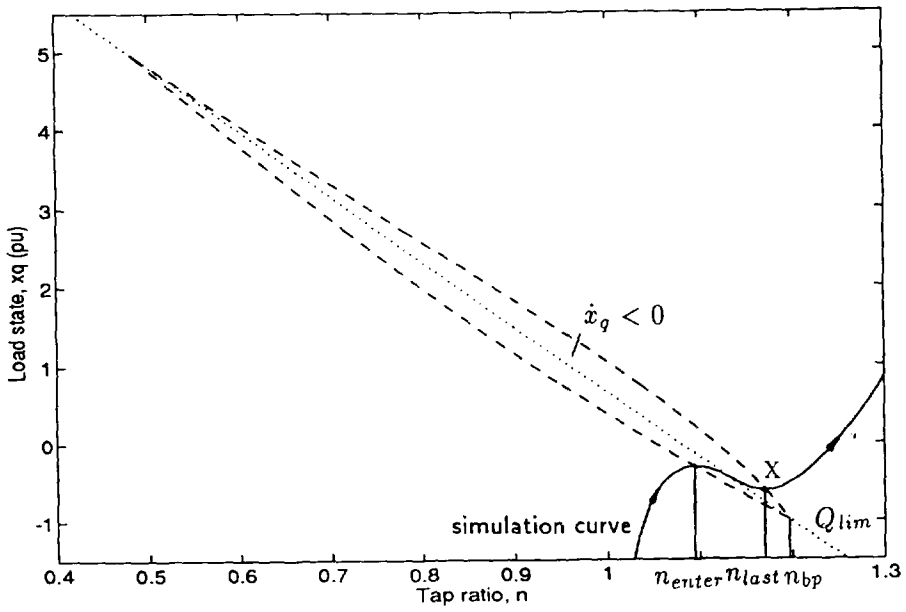

Figure 12. Region $\dot{x}_q < 0$ and voltage collapse scenario as viewed in the n–x_q plane; $Q_s(V) = 0.68 - 0.28V + 0.2V^2$, $Q_{lim} = 0.755$

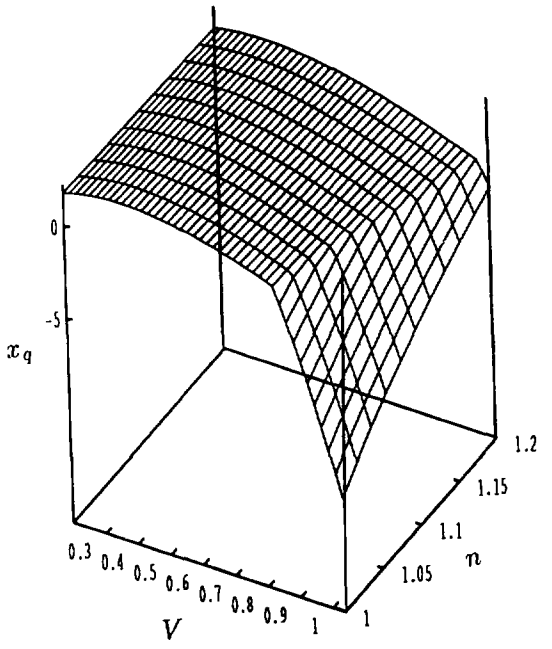

Figure 13. Constraint manifold as viewed in the (V, n, x_q) plane; $Q_s(V) = 0.68 - 0.28V + 0.2V^2$, $Q_{\text{lim}} = 0.74$

limit is encountered voltage steadily declines, leading to a voltage collapse-type situation. This view confirms the observations of the previous part of this sub-section, and will be used to demonstrate the voltage control action in the following section.

V. Alleviating voltage collapse by tap changer control

V.1 *Tap locking strategies*

This section focuses upon some possible control actions, particularly tap changer locking, for preserving the load voltage. In Section III, where the load model did not account for load recovery, it was shown that tap locking should take place when the system trajectory was inside the region of increasing load voltage. However, using the more general load model of Section IV, with x_q now a dynamic state of the system, we will see that the load voltage can be preserved even if the tap is locked at a point outside the $\dot{x}_q < 0$ region. Therefore, detailed analysis of the appropriate time to lock the tap should be made. Depending on the system trajectory behaviour during voltage collapse, there are two cases to consider.

Case 1. Locking the tap while x_q trajectory is inside the excess load region

This decision is shown as always useful. Note that locking the tap means that tap ratio n becomes fixed. Referring to (36), voltage dynamics are then given by

$$\dot{V} = -T_q^{-1} \frac{1}{\dfrac{\partial(Q_t - Q_l)}{\partial V} - \dfrac{\partial Q_l}{\partial E}\dfrac{\partial E}{\partial V}} \dot{x}_q \tag{37}$$

Since locking will not influence the signs of $\dot{x}_q$ and $[(\partial(Q_t - Q)/\partial V - (\partial Q_l/\partial E)(\partial E/\partial V)]$, $\dot{x}_q$ will remain negative and $[(\partial(Q_t - Q_l)/\partial V) - (\partial Q_l/\partial E)(\partial E/\partial V)]$ positive. Then according to (37), $\dot{V}$ becomes positive and load voltage increases.

If, at the moment of locking, the trajectory has not crossed the limit curve, then the trajectory will continue moving vertically downward and will approach the boundary $\dot{x}_q = 0$. The system reaches a stable equilibrium, as shown in Figure 15. Note that the corresponding (uncontrolled) voltage collapse behaviour, i.e., voltage collapse without tap locking, is given in Figure 11.

If, at the moment of locking, the trajectory has already crossed the limit curve, so that $E < E_0$, then from (31) it follows that increasing of voltage V causes the generator terminal voltage E to increase. As the voltage recovers, the system may pass through the Q_{lim} curve again, indicating that the generator had come off its limit, and E had recovered to E_0. Ultimately the system trajectory will reach the $\dot{x}_q = 0$ boundary. At that point, V will become zero, and the system will reach steady state. Alternatively, the Q_{lim} curve may not be encountered

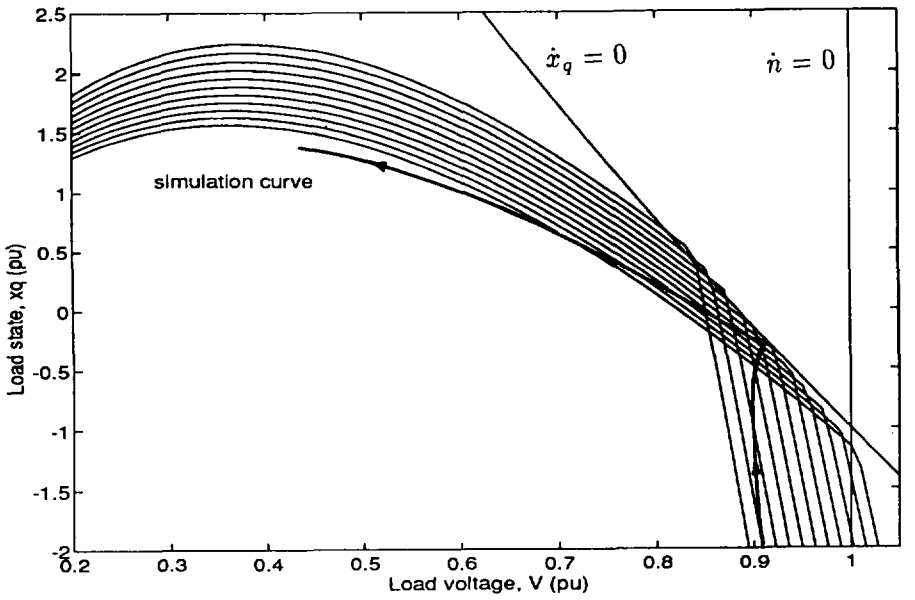

Figure 14. Voltage collapse scenario as viewed in the V–x_q plane; $Q_s(V) = 0.68 - 0.28V + 0.2V^2$, $Q_{\text{lim}} = 0.74$

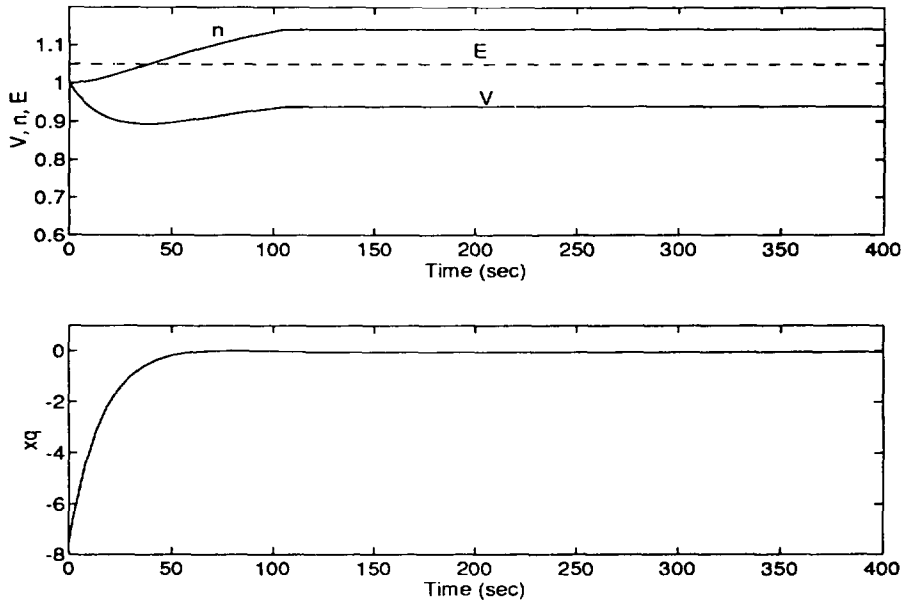

Figure 15. Tap locking while the trajectory is inside the $\dot{x}_q < 0$ region and has not crossed Q_{lim} curve; $Q_s(V) = 0.4 + 0.1V + 0.15V^{2.4}$, $Q_{\text{lim}} = 0.8$; $t_{\text{lok}} = 105$ s

along this post-locking path. Then $E < E_0$ when the trajectory reaches the $\dot{x}_q = 0$ boundary, where the system settles to a steady state. This situation occurs if tap locking for the case considered in Figure 15 is delayed by 15 s, to $t_{\text{lok}} = 120$ s. Again, the corresponding uncontrolled voltage collapse behaviour is given in Figure 11.

Case 2. Locking the tap while x_q trajectory is outside the excess load region

As seen from Figures 10, 11 and 12, the system trajectory which describes the uncontrolled voltage collapse situation has after some time left the $\dot{x}_q < 0$ region. In the case of Figure 8 (or 9) it is obvious that the system trajectory has never entered that region. The decision to lock the tap while the x_q trajectory is outside the $\dot{x}_q < 0$ region may or may not help depending on the time when locking is performed.

Figures 16, 17 and 18 illustrate cases where such a decision halted voltage collapse. Further analysis of the situation illustrated in Figure 17 shows that even later tap locking would have preserved the load voltage. However, exploration of the cases corresponding to Figures 8 (or 9) and 11 shows that if tap locking is delayed too long, collapse will still occur, but at a slower rate than in the corresponding uncontrolled cases.

In the scenario shown in Figure 16 the load voltage was recovering at the time the tap changer was locked. Figures 17 and 18 illustrate cases where the load voltage was decreasing at the locking time, t_{lok}. As discussed earlier, tap locking will not change the signs of $\dot{x}_q$ and $[(\partial(Q_t - Q_l)/\partial V) - (\partial Q_l/\partial E)(\partial E/\partial V)]$. So from

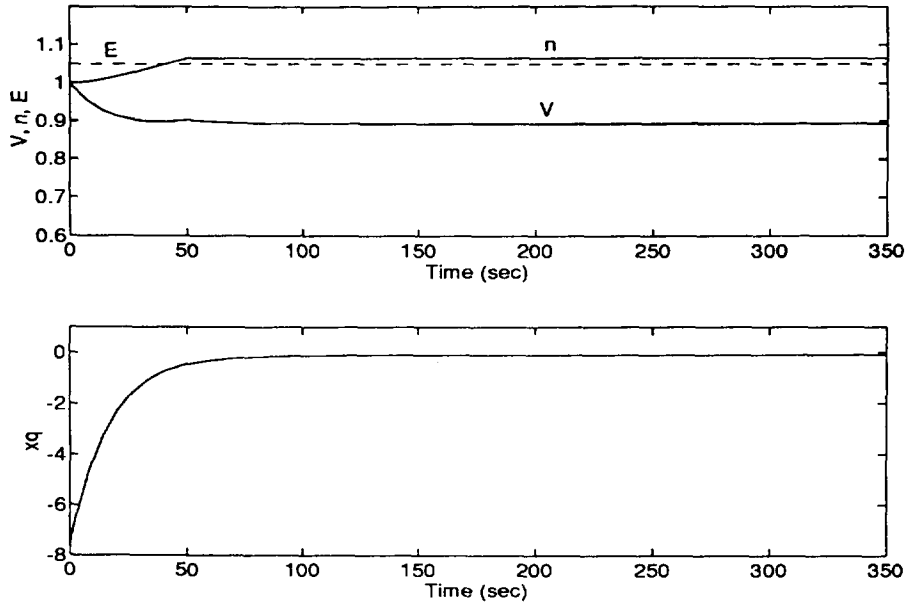

Figure 16. Tap locking while the trajectory is outside the $\dot{x}_q < 0$ region helps; $Q_s(V) = 0.68 - 0.28V + 0.2V^2$, $Q_{\text{lim}} = 0.74$; $t_{\text{lok}} = 50$ s

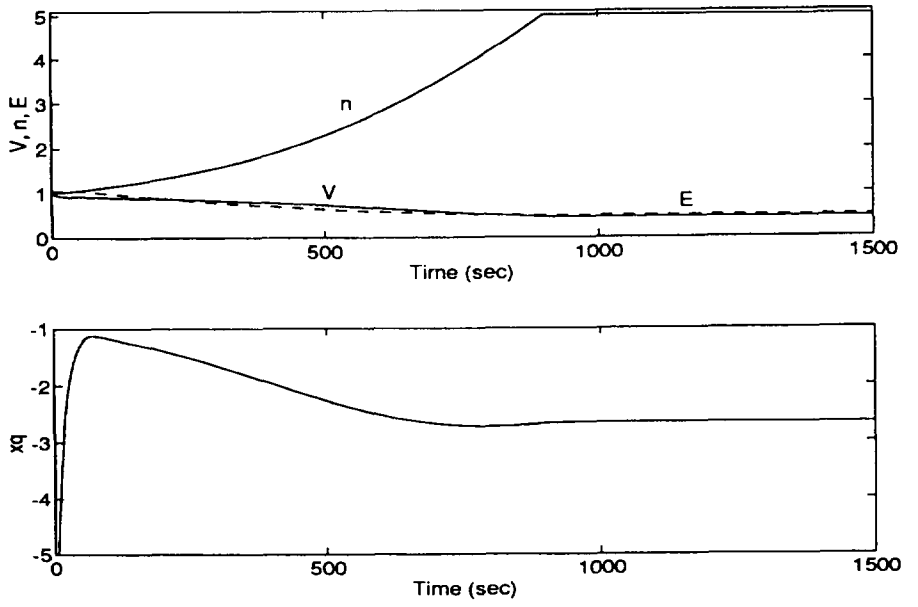

Figure 17. Tap locking performed at $t_{lok} = 900$ s preserves load voltage; $Q_s(V) = 0.65V^{2.1}$, $Q_{lim} = 0.65$

(37), because $\dot{x}_q > 0$, $\dot{V}$ will be negative. However, it is obvious from Figures 16, 17 and 18 that such voltage behaviour immediately after tap locking does not mean that this action does not help. It seems that the sign of $\dot{V}$ does not give an accurate indication of the usefulness of this control action, i.e., there are other factors that need to be taken into account. This issue will be discussed in more detail in the next sub-section.

In the voltage collapse scenarios shown in Figures 8, 10, 11 and 12, it can be seen that if tap locking was performed at any time while the x_q trajectory was below the excess load region, collapse would be avoided. After tap locking, the system trajectory would move vertically upward, ultimately encountering the $\dot{x}_q = 0$ curve. Steady state would be reached at that point.

V.2 *Determination of the latest time to lock the tap changer*

It was shown in Subsection V.1 that locking of the tap while the system trajectory was inside the $\dot{x}_q < 0$ region always resulted in the system reaching a steady state. However, it was also shown that under certain circumstances locking of the tap while the system trajectory was outside that region, or had left the region, could also help. As seen from Figures 17 and 18, where such decisions halted voltage collapse, it means more time to decide to act in order to prevent the collapse.

Detailed analysis of situations shown in Figures 8, 11 and 12 has shown that there is a critical time before which tapping should cease in order to prevent the collapse. Analysis of this critical time problem has pointed out the importance of the system trajectory behaviour.

Referring to Figures 8, 10 and 11, denote the maximum tap ratio for points on the $\dot{x}_q = 0$ boundary by n_{bp}. Since the system trajectory exits the $\dot{x}_q < 0$ region from its low side (Figures 10 and 11) or is passing by it from below (Figure 8), locking the tap at any point up to n_{bp} means

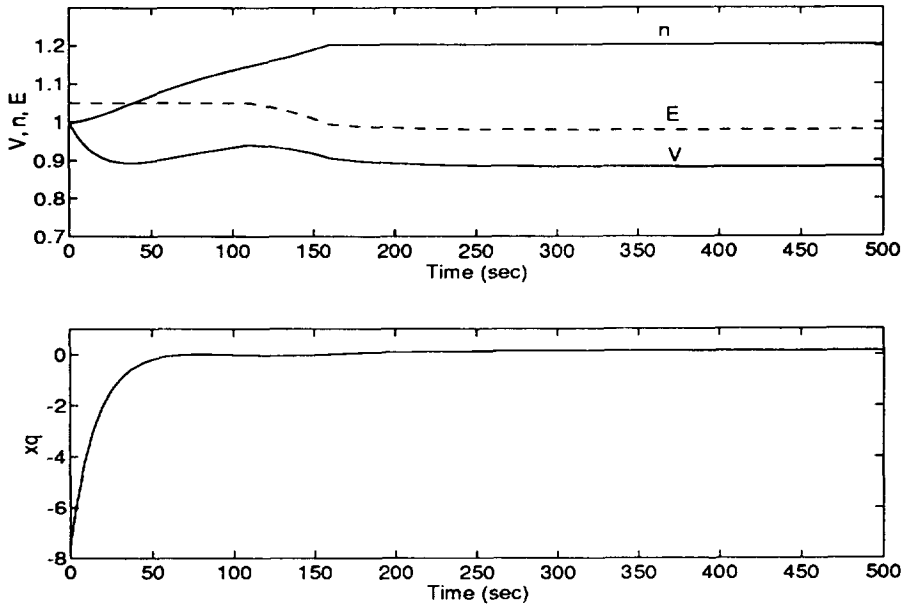

Figure 18. Tap locking performed at $t_{lok} = 160$ s helps; $Q_s(V) = 0.4 + 0.1V + 0.15V^{2.4}$, $Q_{lim} = 0.8$

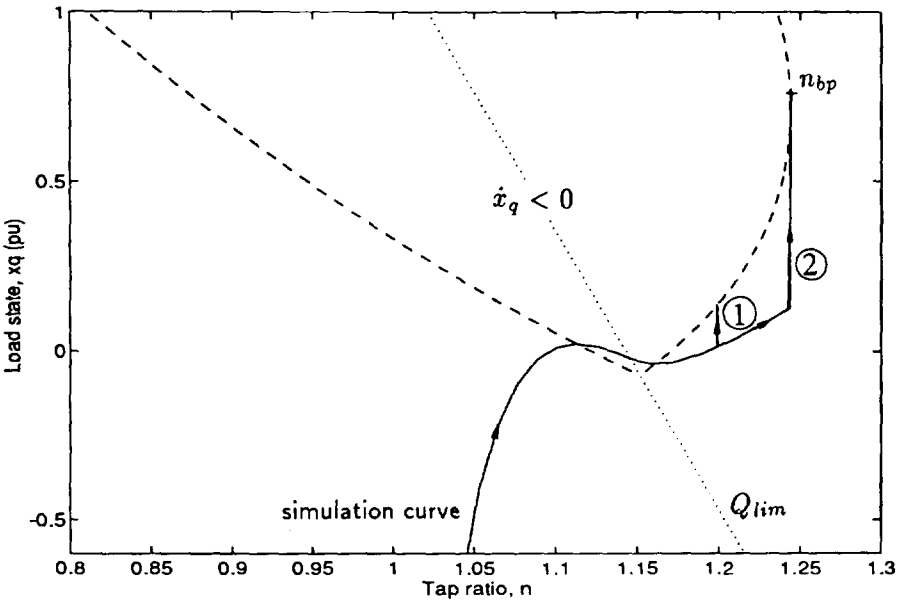

Figure 19. Tap locking performed at $t_{lok} = 160$ s (Curve 1) and at critical time $t_{lok} = 182.7$ s (Curve 2); $Q_s(V) = 0.4 + 0.1V + 0.15V^{2.4}$, $Q_{lim} = 0.8$

that the trajectory on its subsequent vertically upward movement will encounter the $\dot{x}_q = 0$ boundary and stop. The tap locking strategy of Figure 18, given in the n–x_q plane in Figure 19, curve 1, illustrates this behaviour. Alternatively, the corresponding picture in the V–x_q plane is shown in Figure 20. It can be seen that the system trajectory in the V–x_q plane stops at the point of intersection of the constraint manifold, i.e., a contour of fixed n ($n = n(t_{lok})$), and the $\dot{x}_q = 0$ curve. For such fixed n, this intersection point is one of the solution points defined by solving (27), (31) and (32). Figure 21 gives the view in the V–x_q plane of the collapse scenario which results when tap locking occurs too late. It illustrates the case where this intersection point does not exist, and therefore tap locking performed at time t_{lok} would not help. Referring to Figure 19, it means that $n(t_{lok} = 200 \text{ s}) > n_{bp}$. The trajectory on its vertically upward movement does not meet the $\dot{x}_q = 0$ boundary.

From Figure 19, it can be seen that in this case the critical value of tap n_{bp} corresponds to a saddle node bifurcation point. For values of tap less than n_{bp}, points on the $\dot{x}_q = 0$ curve exist. For tap values greater than n_{bp}, no points exist. This is not always the case though, and in some situations n_{bp} is not the appropriate value to lock taps at. The various cases are considered below. We shall refer to the latest value of tap for which locking will be successful as n_{last}.

Case 1. Critical value of tap position is determined as a saddle-node bifurcation point

The critical value of tap position n_{last} is obtained as a

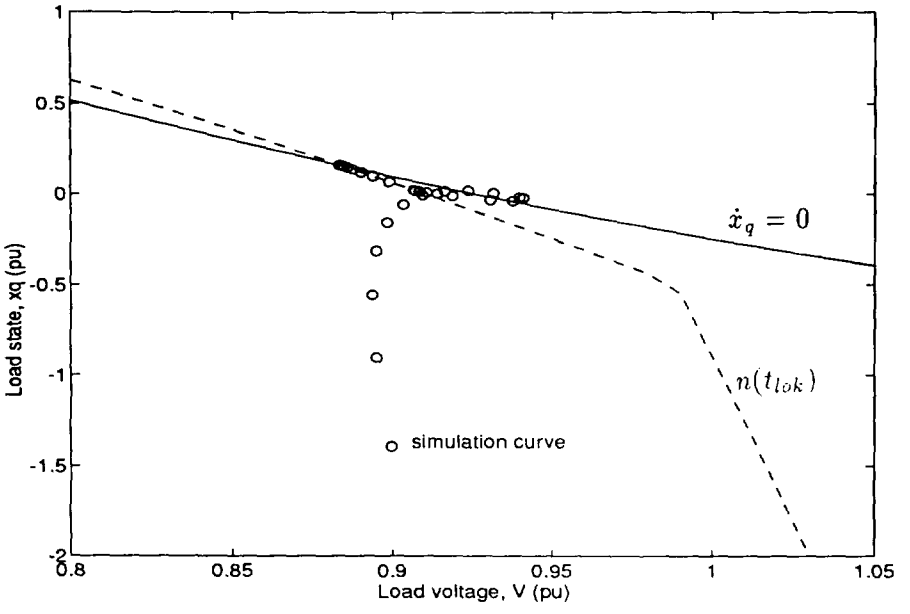

Figure 20. Tap locking performed at $t_{lok} = 160$ s as viewed in the V–x_q plane; $Q_s(V) = 0.4 + 0.1V + 0.15V^{2.4}$, $Q_{lim} = 0.8$

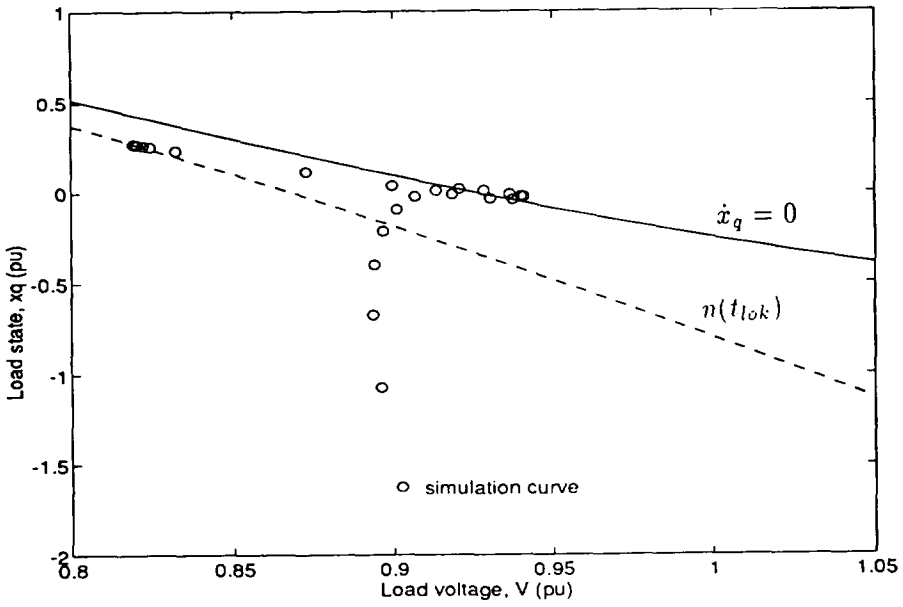

Figure 21. Tap locking performed at $t_{lok} = 200$ s as viewed in the V–x_q plane; $Q_s(V) = 0.4 + 0.1V + 0.15V^{2.4}$, $Q_{lim} = 0.8$

solution of the following set of equations:

$$\dot{E} = E_0 \qquad \text{if } Q_g(E_0) \leqslant Q_{lim}$$

$$Q_g(E) = Q_{lim} \text{ if } Q_g(E_0) > Q_{lim} \Leftrightarrow 0 = f_1(V, n, E) \quad (38)$$

$$0 = -T_q^{-1} x_q + Q_s(V) - Q_t(V) \Leftrightarrow 0 = f_2(V, x_q) \quad (39)$$

$$0 = -Q_l(V, n, E) + T_q^{-1} x_q + Q_t(V) \Leftrightarrow 0 = f_3(V, n, E, x_q) \quad (40)$$

$$0 = \det \begin{bmatrix} \frac{\partial f_1}{\partial V} & \frac{\partial f_1}{\partial x_q} & \frac{\partial f_1}{\partial E} \\ \frac{\partial f_2}{\partial V} & \frac{\partial f_2}{\partial x_q} & \frac{\partial f_2}{\partial E} \\ \frac{\partial f_3}{\partial V} & \frac{\partial f_3}{\partial x_q} & \frac{\partial f_3}{\partial E} \end{bmatrix} \quad (41)$$

In this case, $n_{last} = n_{bp}$. We see from Figure 19, Curve 2 that the system trajectory will just touch the $\dot{x}_q = 0$ boundary curve. In Figure 22 it is shown that this case corresponds to the constraint manifold for $n = n_{last}$ being tangential to the $\dot{x}_q = 0$ curve. Compare this situation with the scenarios of Figures 20 and 21.

Case 2. Critical value of tap position corresponds to a limit induced bifurcation point

This case is illustrated in Figure 8. The bifurcation point occurs at the intersection of the boundary $\dot{x}_q = 0$ and the limit curve Q_{lim}. Because of that, this is called a limit induced bifurcation point. Tap locking will be successful provided it occurs before the tap increases above the value n_{last} given by,

$$0 = Q_g(V, n, E_0) - Q_{lim} \Leftrightarrow 0 = f_1(V, n, E) \quad (42)$$

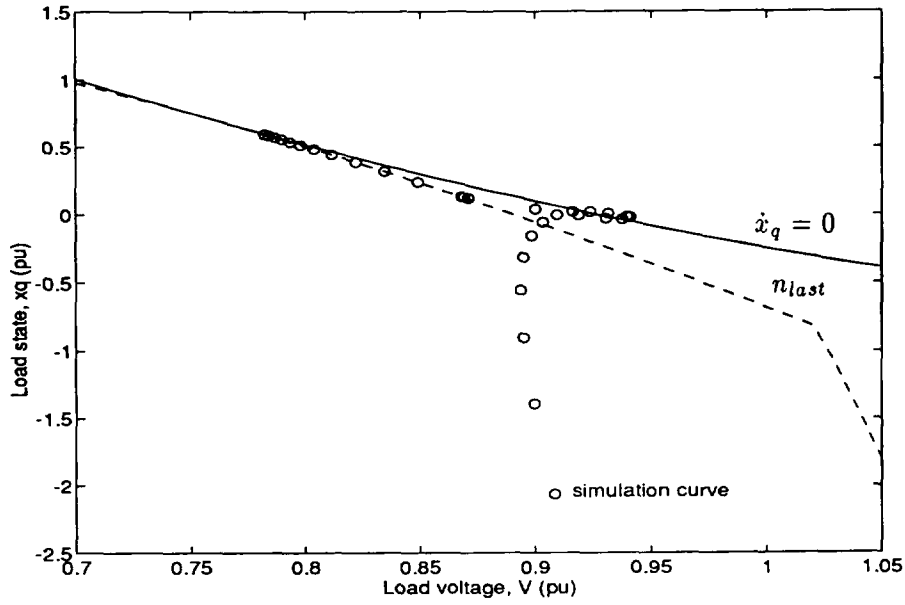

Figure 22. Tap locking performed at critical time ($t_{lok} = 182.7$ s)

$$0 = -T_q^{-1}x_q + Q_s(V) - Q_t(V) \Leftrightarrow 0 = f_2(V, x_q) \quad (43)$$

$$0 = -Q_l(V, n, E_0) + T_q^{-1}x_q + Q_t(V) \Leftrightarrow 0 = f_3(V, n, E, x_q) \quad (44)$$

Case 3. Bifurcation point does not exist

Situations can occur where neither saddle nor limit induced bifurcations occur. This is closely related to the choice of parameters of the static load model $Q_s(V)^{4.14}$. Figure 10 illustrates such a case. Tap locking is always successful in this case. If the trajectory is above the $\dot{x}_q = 0$ curve, then locking will cause the trajectory to move vertically downward and intersect this curve. If the trajectory is below the $\dot{x}_q = 0$ curve, tap locking will result in the trajectory moving vertically upwards, and again reaching a steady state at the intersection with the $\dot{x}_q = 0$ curve.

Case 4. Bifurcation point exists, but it does not determine the critical value of tap position

The case is characteristic of voltage collapse situations where the system trajectory exits the excess load region from its upper side, i.e., above the bifurcation point. This is illustrated in Figure 12. Since outside that region the trajectory has to go up, it is directed away from the boundary. Therefore, performing the tap locking at any time after the trajectory has left the region would have no useful effect. It means that in such a situation, the latest time to lock the tap corresponds to the exit point of the excess load region (point X in Figure 12). Since the position of this point is greatly influenced by the dynamics of the system, it is hard to determine analytically the corresponding values of V, n, x_q and $E < E_0$ at that point. Referring to Figure 12, it is only possible to make the following observation regarding the values of n and x_q:

$$n_{\text{enter}} < n_{\text{last}} < n_{bp}$$

$$x_q(n_{\text{enter}}) > x_q(n_{\text{last}}) > x_q(n_{bp})$$

This case clearly demonstrates the importance of the dynamic behaviour of voltage collapse and the need to establish the link between bifurcation based static and simulation based dynamic approaches.

VI. Conclusion

The paper has investigated long term mechanisms of voltage collapse using recently developed dynamic load models. It is shown that load dynamics, reactive power limiting and tap changing can significantly influence the voltage behaviour. With a dynamic load model[7], the voltage collapse phenomenon is analysed by examining the dynamic interaction between the loads and their supply network. It is shown that appropriate (recovery) load modelling has a significant effect on the decision when the tap changer should be locked in order to alleviate voltage collapse. The results obtained with regard to determining the latest time to lock the tap changer are related to the so-called excess load region, i.e., the region where the load demand is (transiently) greater than the steady state load requirement, and they could be summarized as follows.

- Where the system trajectory passes below, or exits from the low side, of the excess load region, then a bifurcation point of the system equations determines the latest acceptable tap ratio.
- Non-existence of a bifurcation point means that tap locking can be performed at any time.
- Where the system trajectory exits from the upper side of the excess load region, the exit point is the last opportunity to lock taps. Later tap locking will not alleviate voltage collapse.

Illustrations throughout the paper have been based on examples where load recovery was faster than tap changing. However the results of the paper are not dependent on any relationship between load and tap changer time constants. In fact, slower load recovery would lead to a reduced possibility of the system trajectory exiting the excess load region from the upper side. So in cases of slow load recovery, it is more likely that the latest tap locking time can be determined analytically.

The analysis has been undertaken using the continuous-time model of tap changing. Modelling discrete tapping will not affect the above observations, except that it would be more appropriate to talk of the latest time interval to lock the tap in order to preserve the system.

A main result from a practical viewpoint is the inadequacy of using the load voltage (or load voltage derivative) behaviour as an indicator of the control action needed to alleviate voltage collapse.

Even though the studied network is very simple, the results are interesting, since they emphasize the dynamical character of the phenomenon. Studies of more complex networks have been initiated; more general analysis and results are expected to follow.

VII. Acknowledgement

The authors wish to acknowledge the financial support of the Australian Electricity Supply Industry Research Board.

VIII. References

1 *Proc. of the NSF International Workshop on Bulk Power System Voltage Phenomena—II* Deep Creek Lake, Maryland (1991)

2 **Lachs, W** 'Voltage collapse in EHV power systems' *IEEE Paper A* 78 057-2 (1978)

3 **Vu, K T and Liu, C C** 'Shrinking stability regions and voltage collapse in power systems' *IEEE Trans. Circ. Syst.* Vol 39 No 4 (1992) pp 271–289

4 **Hiskens, I A and Hill, D J** 'Dynamic interaction between tapping transformers' *Proc. 11th Power System Computation Conference*, Avignon, France (1993)

5 **Vu, K T and Liu, C C** 'Dynamic mechanisms of voltage collapse' *Syst. Control Letters* Vol 15 (1990) pp 329–338

6 **Van Cutsem, Th** 'Dynamic and static aspects of voltage collapse' *Proceedings of International Workshop on Bulk Power System Voltage Phenomena: Voltage Stability and Security*, Potosi, Missouri (1988)

7 **Hill, D J** 'Nonlinear dynamic load models with recovery for voltage stability studies' *IEEE Trans. Power Syst.* Vol 8 No 1 (1993)

8 **Karlsson, D and Hill, D J** 'Modeling and identification of

nonlinear dynamic loads in power systems' *IEEE Trans. Power Syst.* Vol 9 No 1 (1994) pp 157–166

9 **Mansour, Y** (Ed) 'Voltage stability of power systems: concepts, analytical tools, and industry experiences *IEEE Task Force Report*, Publication 90 TH 0358-2-PWR

10 **Medanić, J, Ilić-Spong, M and Christensen, J** 'Discrete models of slow voltage dynamics for under-load tap changing transformer coordination' *IEEE Trans. Power Syst.* (1987) pp 873–882

11 **Hill, D J, Hiskens, I A and Popović, D** 'Stability analysis of load systems with recovery dynamics' *Int. J. Electr. Power Energy Syst.*, Vol 16 No 4 (1994) pp 277–286

12 **Xu, W and Mansour, Y** 'Voltage stability analysis using generic dynamic load models' *IEEE Trans. Power Syst.* Vol 9 No 1 (1994) pp 479–493

13 **Walve, K** 'Modeling of power system components at severe disturbances' *CIGRE Report* 38–18 (1986)

14 **Hiskens, I A and Hill, D J** 'Modelling of dynamic load behaviour' *Proc. of the NSF Workshop on Bulk Power System Voltage Phenomena—III: Voltage Stability, Security and Control* Davos, Switzerland (1994)

15 **Popović, D, Hiskens, I A and Hill, D J** 'Investigations of load-tap changer interaction' *University of Newcastle Technical Report* EE9382 (1994) (revised)

16 **Hill, D J, Hiskens, I A and Popović, D** 'Load recovery in voltage stability analysis and control' *Proc. of the NSF Workshop on Bulk Power System Voltage Phenomena—III: Voltage Stability, Security and Control* Davos, Switzerland (1994)

Appendix

For the system in Figure 1, the derivatives in (36) are given by,

$$\frac{\partial Q_l}{\partial V} = \frac{1}{nX}\left(E - 2\frac{V}{n}\right) \tag{45}$$

$$\frac{\partial Q_l}{\partial n} = \frac{V}{n^2 X}\left(2\frac{V}{n} - E\right) \tag{46}$$

$$\frac{\partial Q_l}{\partial E} = \frac{V}{nX} \tag{47}$$

$$\frac{\partial E}{\partial V} = \frac{1}{2n}\left(1 + \frac{V}{n\sqrt{\frac{V^2}{n^2} + 4Q_{\lim}X}}\right) \tag{48}$$

$$\frac{\partial E}{\partial n} = -\frac{V}{2n^2}\left(1 + \frac{V}{n\sqrt{\frac{V^2}{n^2} + 4Q_{\lim}X}}\right) \tag{49}$$

It is obvious that $\partial Q_l/\partial E$ and $\partial E/\partial V$ are always positive, whilst $\partial E/\partial n$ is always negative. Considering some reasonable values of V, n, E, derivative $\partial Q_l/\partial n$ is positive, and $\partial Q_l/\partial V$ is negative. Consider the signs of the terms given in (36), $[(\partial(Q_t - Q_l)/\partial V) - (\partial Q_l/\partial E)(\partial E/\partial V)]$ and $[(\partial(Q_t - Q_l)/\partial n) - (\partial Q_l/\partial E)(\partial E/\partial n)]$. After some algebraic manipulation of (45)–(49) we find

$$\frac{\partial(Q_t - Q_l)}{\partial V} - \frac{\partial Q_l}{\partial E}\frac{\partial E}{\partial V} = \frac{k_q}{T_q} + \frac{1}{nX}\left[\frac{V}{2n}\left(3 - \frac{V}{n\sqrt{\frac{V^2}{n^2} + 4Q_{\lim}X}}\right) - E\right] \tag{50}$$

$$\frac{\partial(Q_t - Q_l)}{\partial n} - \frac{\partial Q_l}{\partial E}\frac{\partial E}{\partial n} = -\frac{V}{n^2 X}\left[\frac{V}{2n}\left(3 - \frac{V}{n\sqrt{\frac{V^2}{n^2} + 4Q_{\lim}X}}\right) - E\right] \tag{51}$$

Since the analysed voltage collapse situations are characterized by low V and high n, i.e., $V/n < 1$, and $V/[n\sqrt{(V^2/n^2) + 4Q_{\lim}X}]$ is also less than 1, and the whole term given in brackets is negative, assuming that the value of E is not significantly less than E_0; it means that $[(\partial(Q_t - Q_l)/\partial n) - (\partial Q_l/\partial E)(\partial E/\partial n)]$ is positive. Also, for some chosen values of k_q, T_q in (50), $k_q/T_q > (1/nX)[(V/2n)(3 - V/[n\sqrt{(V^2/n^2) + 4Q_{\lim}X}]) - E]$, so that $[(\partial(Q_t - Q_l)/\partial V) - (\partial Q_l/\partial E)(\partial E/\partial V)]$ is also positive.